

A NOVEL LOSS COMPENSATION TECHNIQUE FOR HIGH-Q BROAD-BAND ACTIVE INDUCTORS

Hitoshi Hayashi, Masahiro Muraguchi,
Yohtaro Umeda and Takatomo Enoki

NTT Wireless Systems Laboratories
1-2356 Take, Yokosuka-shi, Kanagawa 238-03, Japan

ABSTRACT

A novel loss compensation technique for high-Q broad-band active inductors is proposed. This yields frequency-insensitive negative resistance to compensate constant internal losses. Measured frequency range is 6 to 20 GHz for Q values greater than 100, and 7 to 15 GHz for Q values greater than 1,000.

INTRODUCTION

Active inductors suffer significant constant internal loss due to several factors such as the drain-to-source conductance of the FET and the DC bias circuit. Several remedies have been introduced [1]-[7], including some attractive approaches that achieve high-Q values by using negative resistance. However, our simplified equivalent circuit analysis revealed that these techniques result in limited band characteristics. If the negative resistance generated in series with the inductance could be made constant against the operating frequency, the loss could be canceled over a much wider frequency band, i.e., from DC to the microwave frequency range.

This paper proposes a technique for high-Q broad-band active inductors in which the circuit structure generates frequency-insensitive negative resistance that almost completely compensates the constant internal loss. This yields a much wider frequency band than offered with previously reported active inductors.

DESIGN APPROACH

The schematic of a previously reported active inductor (P-A type) is shown in Fig. 1(a) [1]. This circuit is composed of common-source cascode FETs (FET1 and FET2) and common-gate cascode FETs (FET3 and FET4) feedback. Shunt resistor R0

is connected parallel to the output port. If the FET equivalent circuit is assumed to be just a combination of the transconductance gm and the gate-to-source capacitance C_{gs} , and the FETs have the same cut-off frequency f_T ($= gm/2\pi C_{gs}$), the simplified equivalent circuit obtained from our analysis is as shown in Fig. 1(b). The internal loss R_i , caused by the drain-to-source conductance of the FETs, the resistors for DC bias, and several other factors, is almost constant at the operating frequency range below $f_T/2$ experimentally. The total series resistance varies against the operating frequency because the negative resistance is parallel to inductance. Thus, R_i can be canceled by adjusting the amounts of R_0 and gm^3 against the operating frequency.

Another previously reported active inductor (P-B type) is based on a combination of a common-source FET (FET1) and a feedback common-gate FET (FET2), as shown in Fig. 2(a) [5]. Shunt resistor R_0 is connected between the ground and the gate of FET2. The simplified equivalent circuit obtained from our analysis is shown in Fig. 2(b). The total series resistance varies with the frequency because the generated negative resistance is proportional to the square of the frequency. Thus, R_i can be canceled by adjusting the amounts of R_0 and gm^2 against the operating frequency.

In these two methods, the following facts were overlooked: If the negative resistance generated in series with the inductance could be made constant against the operating frequency, the loss could be canceled over a much wider frequency band, i.e., from DC to the microwave frequency range. A schematic of this new inductor is shown in Fig. 3(a). The gate of FET3 is connected to the drain of FET1 and the source of FET2, and resistor R_0 is connected between the drain of FET2 and the output port. A simplified equivalent circuit is shown in Fig. 3(b). Note that the negative resistance shows no frequency term so R_i can be fully canceled by adjusting the amounts of R_0 and gm^2 for the entire frequency range. Furthermore, this circuit has a higher inductance

value than previously reported circuits according to our analysis.

EXPERIMENTAL RESULTS

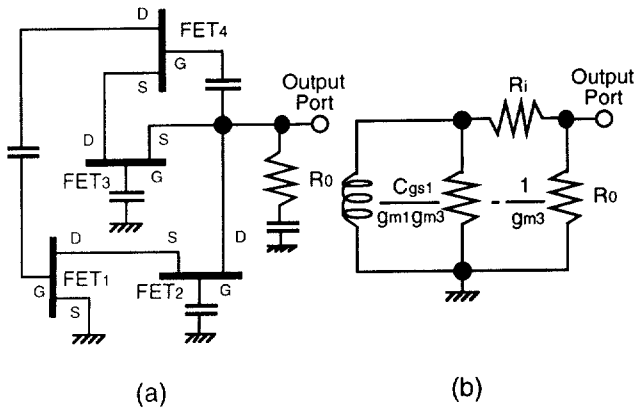


Fig. 1 Type P-A active inductor.
(a) circuit configuration
(b) simplified equivalent circuit

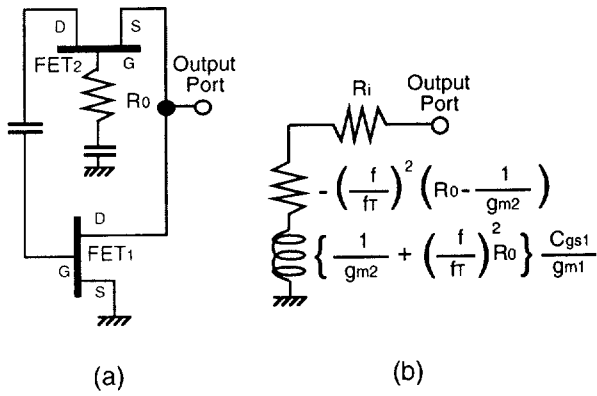


Fig. 2 Type P-B active inductor.
(a) circuit configuration
(b) simplified equivalent circuit

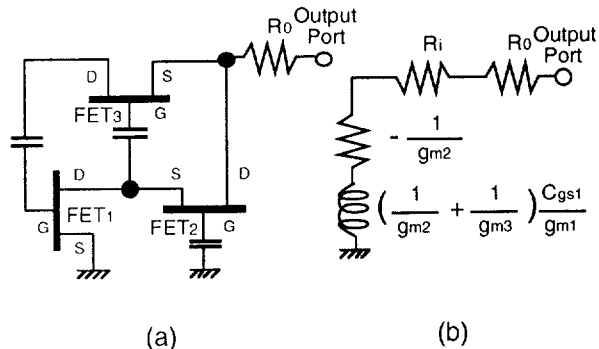


Fig. 3 Proposed active inductor.
(a) circuit configuration
(b) simplified equivalent circuit

The experimental active inductor is shown in Fig. 4. The inductor was fabricated using four 0.1- μm -gate-length InAlAs/InGaAs/InP HEMTs [8] for FET1, FET2, FET3, FET4 (DC biasing FET). The HEMTs are 25 μm wide and feature nonalloyed ohmic contacts for the source and drain electrodes. To reduce the contact resistance, a novel n⁺-InGaAs/n⁺-InAlAs cap layer was used. The HEMTs have an average f_T of 140 GHz and f_{max} of 180 GHz. The resistor R₀ is 29 Ω . A photograph of the MMIC chip is shown in Fig. 5. The chip size is 0.4 x 0.78 mm².

The measured S parameters from 2 to 26 GHz are shown in Fig. 6. The associated series resistance is kept above 0 Ω in the

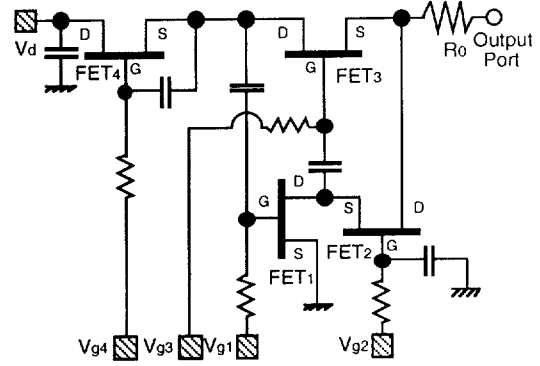


Fig. 4 Detailed schematic of the experimental active inductor.

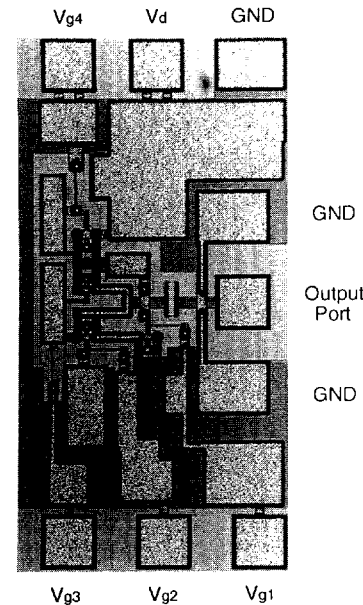


Fig. 5 Photograph of the MMIC chip.

frequency range of 0.045 GHz through 26.5 GHz by the appropriate bias conditions, $V_{g1} = 0.0$ V, $V_{g2} = 1.2$ V, $V_{g3} = 2.4$ V, $V_{g4} = 3.5$ V, $V_d = 4.9$ V, and $I_d = 11$ mA. This shows that loss compensation is obtained up to more than 20 GHz. The measured S parameters at 2 GHz are capacitive because of the DC cut capacitors. Figure 7 shows the measured impedance-frequency characteristics, where the impedance is represented by series resistance and inductance. The inductance values at 6 GHz and 20 GHz are respectively 0.41 nH and 0.82 nH, and the Q value in this frequency range is greater than 100. The inductance values

at 7 GHz and 15 GHz are respectively 0.44 nH and 0.59 nH, and the Q value in this frequency range is greater than 1,000. The low-loss and wide-band characteristics are due to the proposed constant series negative resistance compensation.

Considering applications for active filters, phase shifters, oscillators and so forth, one of the most important problems is stability against temperature variation. Figure 8 shows measured impedance-frequency characteristics when the temperature is varied from -5 $^{\circ}$ C to 55 $^{\circ}$ C. The variation of the inductance and resistance values at 18 GHz are respectively within 0.1 nH and 2 Ω .

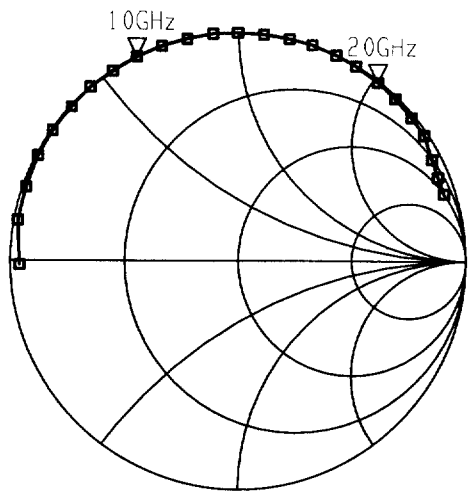


Fig. 6 Measured S parameters of the experimental circuit.

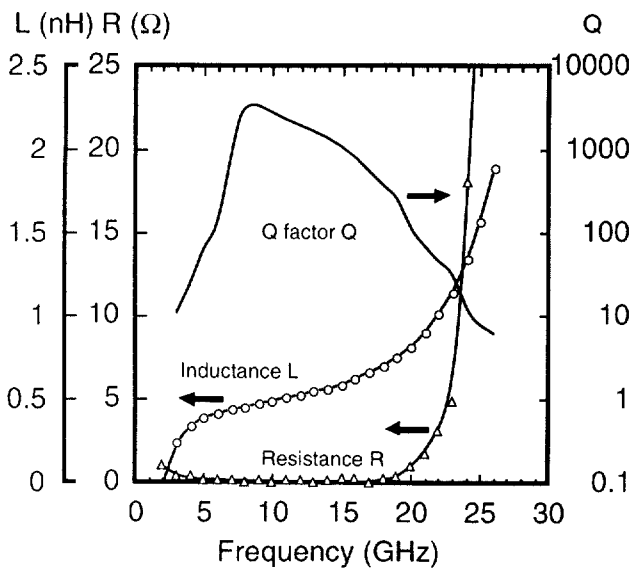
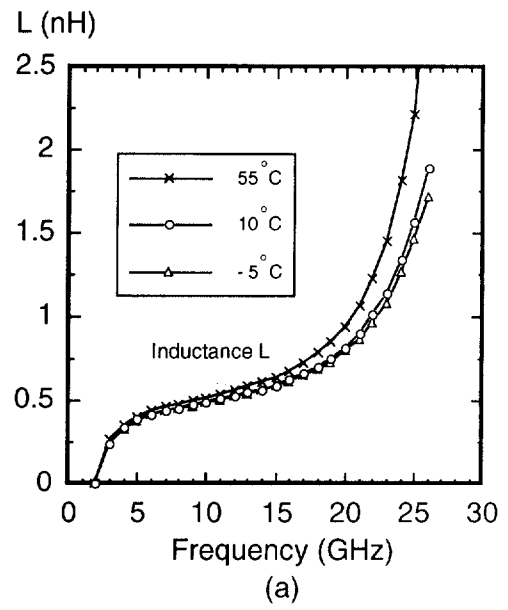


Fig. 7 Measured impedance-frequency characteristics of the experimental active inductor.



(a)

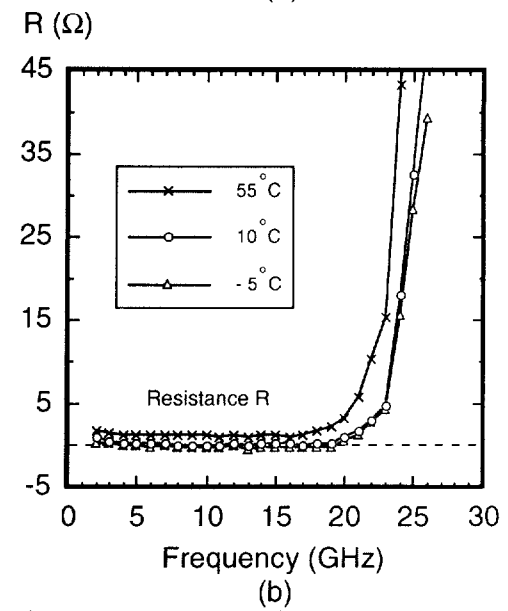


Fig. 8 Measured impedance-frequency characteristics with temperature variation.

The input-output characteristics at the frequency of 8 GHz was measured to investigate dynamic range. The test setup for measuring linearity is shown in Fig. 9. A 8 GHz signal was injected into the active inductor through a circulator, and the reflected signal was observed by a spectrum analyzer. The 1-dB gain compression point is -1 dBm of incident power, and the fundamental power to the second-harmonic wave power of the reflected signal is more than 20 dB, as shown in Fig. 10. The phase deviation is less than 1 degree in this incident power range, which means that the variation of the inductance and resistance values are negligible up to -1 dBm of input power.

CONCLUSION

A novel loss compensation technique for high-Q broad-band active inductors has been proposed. This generates frequency-insensitive negative resistance in series with inductance to compensate constant internal losses. The experimental active inductor covers a measured frequency range of 6 to 20 GHz for Q values greater than 100, and 7 to 15 GHz for Q values greater than 1,000.

This technique is highly desirable for achieving high-performance filters, VCOs and analog phase shifters.

ACKNOWLEDGMENT

We wish to thank Mr. A. Hashimoto, Dr. M. Aikawa and Mr. T. Tokumitsu for their many helpful discussions and encouragement.

REFERENCES

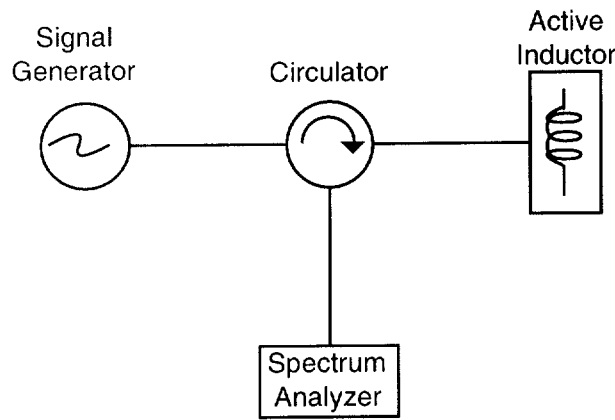


Fig. 9 Block diagram of the test setup for linearity measurement.

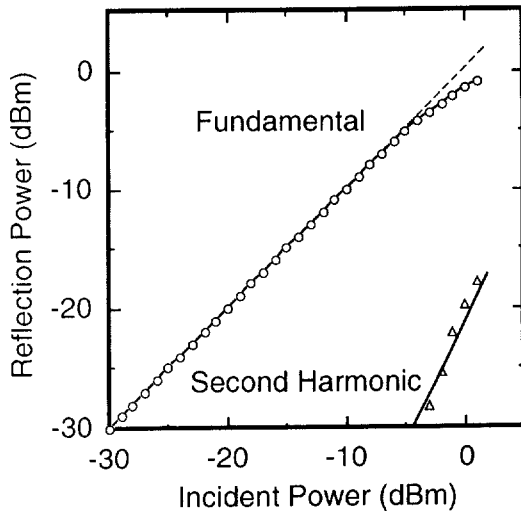


Fig. 10 Reflection power versus incident power.

- [1] S. Hara et al., "Lossless broad-band monolithic microwave active inductors," *IEEE Trans. Microwave Theory Tech.*, vol. 37, pp. 1979-1984, Dec. 1989.
- [2] B. Hopf et al., "Narrow band MMIC active filter using negative resistance circuits in coplanar line technique," *Proc. 25th EuMC*, pp. 1110-1112, 1995.
- [3] G. F. Zhang et al., "New broadband tunable monolithic microwave floating active inductor," *Electron. Lett.*, vol. 28, no. 1, pp. 78-81, 1992.
- [4] C. Zanchi et al., "A tunable lossless HBT broad-band monolithic microwave floating active inductor," *Proc. 24th EuMC*, pp. 793-798, 1994.
- [5] P. Alinikula et al., "Monolithic active resonators for wireless applications," *IEEE Microwave and Millimeter-Wave Monolithic Circuits Symp. Dig.*, pp. 197-200, 1994.
- [6] S. Lucyszyn et al., "Monolithic narrow-band filter using ultrahigh-Q tunable active inductors," *IEEE Trans. Microwave Theory Tech.*, vol. 42, pp. 2617-2622, Dec. 1994.
- [7] E. M. Bastida et al., "GaAs monolithic microwave integrated circuits using broadband tunable active inductors," *Proc. 19th EuMC*, pp. 1282-1287, 1989.
- [8] T. Enoki et al., "0.1-μm InAlAs/InGaAs HEMTs with an InP-recess-ctch stopper grown by MOCVD," *IEEE 7th Int. Conf. on InP and Related Materials Dig.*, Sapporo, Japan, pp. 81-84.